

Determination of Discharge During Pulsating Flow

GEOLOGICAL SURVEY WATER-SUPPLY PAPER 1869-D

*Prepared in cooperation
with the California
Department of Water
Resources*



Determination of Discharge During Pulsating Flow

By T. H. THOMPSON

RIVER HYDRAULICS

GEOLOGICAL SURVEY WATER-SUPPLY PAPER 1869-D

*Prepared in cooperation
with the California
Department of Water
Resources*



UNITED STATES DEPARTMENT OF THE INTERIOR

STEWART L. UDALL, *Secretary*

GEOLOGICAL SURVEY

William T. Pecora, *Director*

CONTENTS

	Page
Abstract.....	D1
Introduction.....	2
Purpose and scope.....	2
Acknowledgments.....	5
Characteristics of pulsating flow.....	5
Determination of discharge.....	6
Description of the Haines Creek instrumentation.....	6
Description of controlled test in Santa Anita Wash.....	7
Method of computing discharge.....	10
Discussion of results.....	15
Proposed methods of determining discharge.....	17
Photographic method.....	17
Depth-recorder method.....	19
Dye-dilution method.....	19
Discussion of proposed methods.....	20
Summary and conclusions.....	21
Selected references.....	22

ILLUSTRATIONS

FIGURE		Page
1.	Index map showing observation sites on Santa Anita Wash in Arcadia, Calif.....	D3
2.	Photograph showing pulsating flow in Santa Anita Wash above Sierra Madre Wash.....	4
3.	Sketch showing dimensions and configuration of grid on channel wall.....	7
4-6.	Discharge hydrographs at observation sites on Santa Anita Wash:	
4.	Above Sierra Madre Wash (O.S. 201).....	9
5.	At Colorado Blvd. (O.S. 202).....	10
6.	At Longden Ave. (O.S. 203).....	11
7.	Schematic sketch of longitudinal water-surface profile and list of elements observed.....	12
8.	Schematic sketch of general component layout for photographic method of determining discharge.....	18

TABLES

TABLE		Page
	1. Channel geometry at observation sites on Santa Anita Wash flood control channel.....	D8
	2. Computation of discharge in the overriding wave (Q_w) at O.S. 201.....	12
	3. Computation of discharge in the shallow-depth (overrun) part of flow (Q_1) and total discharge at O.S. 201.....	13
	4. Computation of discharge in the overriding wave (Q_w) at O.S. 202.....	14
	5. Computation of discharge in the shallow-depth (overrun) part of flow (Q_1) and total discharge at O.S. 202.....	15
	6. Computation of discharge in the overriding wave (Q_w) at O.S. 203.....	15
	7. Computation of discharge in the shallow-depth (overrun) part of flow (Q_1) and total discharge at O.S. 203.....	16
	8. Observed wave characteristics at approximate time of maximum discharge.....	17

SYMBOLS

A_1	Cross-sectional area of channel (ft ²)
b	Width of channel (ft)
D_1	Depth between waves (ft)
D_2	Depth at wave front (ft)
g	Gravitational constant
h_w	Height of wave crest (ft)
L_w	Length of overriding wave from crest to trough (ft)
L_r	Length of measuring reach (ft)
n	Roughness factor (Manning)
Q_1	Discharge in shallow-depth part of flow (cfs)
Q_w	Discharge in overriding wave (cfs)
R	Hydraulic radius (ft)
S	Slope of channel (ft/ft)
t_b	Time interval between arrivals of crest and trough at observation point. (sec)
t_w	Time required for wave crest to travel length of measuring reach (sec)
T_p	Time interval between arrivals of consecutive wave fronts at observation point (sec)
V	Velocity (fps)
V_1	Shallow-depth velocity (fps)
V_w	Average wave velocity (fps)

RIVER HYDRAULICS

DETERMINATION OF DISCHARGE DURING PULSATING FLOW

By T. H. THOMPSON

ABSTRACT

Pulsating flow in an open channel is a manifestation of unstable-flow conditions in which a series of translatory waves of perceptible magnitude develops and moves rapidly downstream. Pulsating flow is a matter of concern in the design and operation of steep-gradient channels. If it should occur at high stages in a channel designed for stable flow, the capacity of the channel may be inadequate at a discharge that is much smaller than that for which the channel was designed. If the overriding translatory wave carries an appreciable part of the total flow, conventional stream-gaging procedures cannot be used to determine the discharge; neither the conventional instrumentation nor conventional methodology is adequate.

A method of determining the discharge during pulsating flow was tested in the Santa Anita Wash flood control channel in Arcadia, Calif., April 16, 1965. Observations of the dimensions and velocities of translatory waves were made during a period of controlled reservoir releases of about 100, 200, and 300 cfs (cubic feet per second). The method of computing discharge was based on (1) computation of the discharge in the overriding waves and (2) computation of the discharge in the shallow-depth, or overrun, part of the flow. Satisfactory results were obtained by this method. However, the procedure used—separating the flow into two components and then treating the shallow-depth component as though it were steady—has no theoretical basis. It is simply an expedient for use until laboratory investigation can provide a satisfactory analytical solution to the problem of computing discharge during pulsating flow.

Sixteen months prior to the test in Santa Anita Wash, a robot camera had been designed and programmed to obtain the data needed to compute discharge by the method described above. The photographic equipment had been installed in Haines Creek flood control channel in Los Angeles, Calif., but it had not been completely tested because of the infrequency of flow in that channel. Because the Santa Anita Wash tests afforded excellent data for analysis, further development of the photographic technique at Haines Creek was discontinued.

Three methods for obtaining the data needed to compute discharge during pulsating flow are proposed. In two of the methods—the photographic method and the depth-recorder method—the dimensions and velocities of translatory waves

are recorded, and discharge is then computed by the procedure developed in this report. The third method—the constant-rate-dye-dilution method—yields the discharge more directly. The discharge is computed from the dye-injection rate and the ratio of the concentration of dye in the injected solution to the concentration of dye in the water sampled at a site downstream. The three methods should be developed and tested in the Santa Anita Wash flood control channel under controlled conditions similar to those in the test of April 1965.

INTRODUCTION

Pulsating flow in an open channel, as defined by Chow (1959, p. 580), is a manifestation of unstable-flow conditions in which a series of translatory waves of perceptible magnitude develops and moves rapidly downstream. These translatory waves, commonly called roll waves or slug flow, are a matter of concern to the designer of steep-gradient channels. Channels are invariably designed for stable flow. Should pulsating flow occur at high stages in a channel so designed, the channel capacity may be inadequate at a discharge much smaller than the design flow.

If the overriding translatory wave carries an appreciable part of the total flow, conventional stream-gaging methods cannot be used to determine the discharge. Conventional water-stage recorders of either the float or pressure-sensing type do not react quickly enough to record the rapidly fluctuating stage; depths and velocities change too rapidly to permit discharge measurement by current meter; no stage-discharge relation exists for pulsating flow; and the commonly used formulas for computing stable open-channel discharge are not applicable.

PURPOSE AND SCOPE

The purpose of the study was twofold: to develop and test a method for computing discharge during pulsating flow and to suggest instrumentation for automatic monitoring of the hydraulic elements needed to compute flow under such conditions of instability.

Pulsating-flow data were obtained by Los Angeles County Flood Control District personnel during observations April 16, 1965, at three observation sites (O.S. 201, O.S. 202, and O.S. 203) on the Santa Anita Wash flood control channel in Arcadia, Calif. (fig. 1). These data were used to test a method of computing discharge that is based on the dimensions of the translatory waves and on the velocity of the wave fronts. The rate of flow was controlled during the test period by releases from the reservoir upstream at Big Santa Anita Dam. Observations were made during rates of release of about 100, 200, and 300 cfs (cubic feet per second). Figure 2 shows pulsating flow at the upstream observation site (O.S. 201) at a discharge of about 200 cfs. The depth

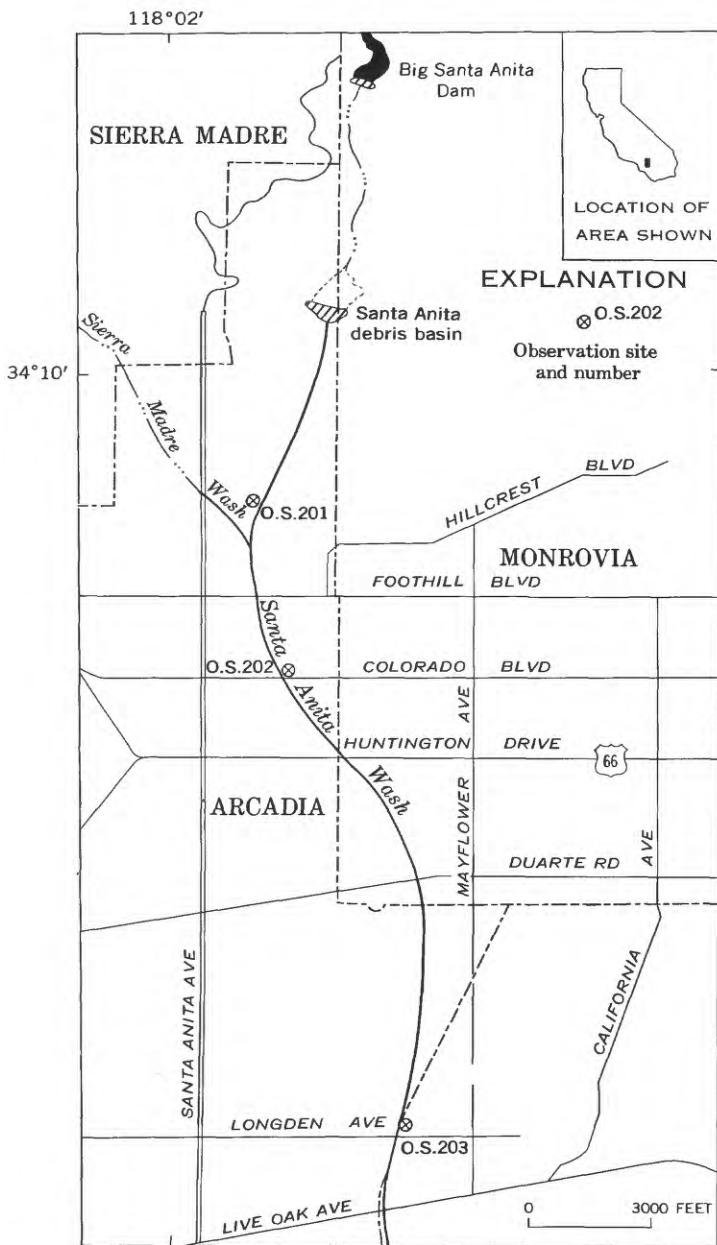


FIGURE 1.—Observation sites on Santa Anita Wash in Arcadia, Calif.

of the water ahead of the wave front at this discharge was 0.25 foot and the total depth of water in the wave front was 0.9 foot.

Prior to this test, efforts had been made to determine discharge during periods of pulsating flow in Haines Creek flood control channel in Los Angeles, by photographically documenting wave dimensions and wave velocities. A prolonged drought, however, afforded few runoff events for observing and testing the photographic equipment. After 16 months of sporadic operation the opportunity for the controlled test on Santa Anita Wash presented itself, and shortly afterwards the camera was removed from the installation at Haines Creek. The instrumentation suggested later in this report was based in part on the experience gained at Haines Creek, but primarily on the observations made during the Santa Anita Wash test and on the subsequent analysis of that data.



FIGURE 2.—Pulsating flow in Santa Anita Wash above Sierra Madre Wash (O.S. 201) in Arcadia, Calif., April 16, 1965. Discharge was about 200 cfs.

ACKNOWLEDGMENTS

This study was made under a cooperative agreement between the U.S. Geological Survey and the State of California, Department of Water Resources. The report was prepared by the Water Resources Division of the Geological Survey, under the general supervision of Walter Hofmann, former district chief for California, and his successor, R. S. Lord. Technical supervision was provided by S. E. Rantz, research hydrologist, who gave helpful advice and guidance during the data analysis and report preparation. The Haines Creek instrumentation was developed and supervised by Winchell Smith, hydrologist.

The valuable assistance and data furnished by the Los Angeles County Flood Control District are gratefully acknowledged.

CHARACTERISTICS OF PULSATING FLOW

Little is known concerning unstable or pulsating flow. From laboratory experiments and field observations many investigators have definitely established that unstable flow will develop only in steep channels. Craya (1952), Vedernikov (Powell, 1948), and others agree that some perturbation or disturbance to stable flow, no matter how slight, is required to trigger instability, and a length of channel downstream is required for pulsating flow to develop. The investigators also believe that the minimum length of channel required for this development depends on the channel geometry and on the degree of instability that the flow has attained on entering the reach of channel. For example, engineers of the Los Angeles County Flood Control District (oral commun., 1965) have observed that large flow disturbances, caused by stream-borne debris lodged in a steep channel, can cause pulsating flow to develop in a very short reach. The length of channel required for the development of pulsating flow also increases with the depth of the flow. Field observations of spectacular examples of pulsating flow have been documented. Holmes (1936) described waves, in steep stormflow channels, whose heights ranged from 5 to 8 feet. The wedge-shaped waves were several hundred feet long, and the channel between waves was dry or nearly so.

Many investigators have derived an index of instability based on laboratory data; that is, a numerical index that describes the conditions required for incipient instability. An obvious index would be based on Froude number; steep slopes are required for instability. Channel geometry has an effect, however, and because flumes in the various laboratories vary in size, almost every investigator has his own index of instability. Koloseus and Davidian (1966) used Froude number and relative roughness; Thomas (1940) and Mayer (1959) used Froude

number and slope; Vedernikov (Powell, 1948) used Froude number and a shape factor; and Escoffier and Boyd (1962) used slope, bottom width, roughness, and discharge.

Observation of the waves in Santa Anita Wash during the field test bears out the statements about the development of pulsating flow. Small perturbations of the water surface originated on the steep spillway of the debris-basin dam at the upstream end of the flood control channel (fig. 1). Perturbations did not grow significantly until the flow became disturbed in a superelevated bend in the channel, 2,000 feet downstream from the dam. In this bend the flow showed the pattern of reflected waves that is typical of all supercritical flows in bends. As the flow passed the bend, pulsating flow became fully developed, and a continuous series of relatively large translatory waves moved down the channel. The wave fronts were perpendicular to the channel walls. The waves were not evenly spaced and occasionally one wave would overtake another, but in general the waves maintained their spacing and underwent little attenuation in the upper 2-mile reach of channel. As the channel became wider and the slope decreased in the lower reach, there was slight attenuation of the waves and the period between waves increased.

DETERMINATION OF DISCHARGE

DESCRIPTION OF THE HAINES CREEK INSTRUMENTATION

The first efforts by the Geological Survey to document and determine discharge during pulsating flow were made from January 1964 to August 1965 in the concrete-lined Haines Creek flood control channel in the Tujunga area of Los Angeles, Calif. Instrumentation at the test site consisted of a 24-mm robot camera mounted so that vertical and horizontal changes in camera position occurred during a programmed cycle. A 200-foot film magazine was used, and the camera operated at a rate of 6 frames per second. The control and power units were housed in a 48-inch corrugated-metal pipe shelter on the left bank, with the camera set in an appended box which projected over the channel. Photographs were taken through windows in the box that faced upstream and across the channel.

A grid, as shown in figure 3, was painted on the channel wall opposite the camera so that water depths could be read. Upstream from the grid, vertical stripes were painted on the wall at 20-foot intervals for a distance of 400 feet so that wave velocities could be computed.

The camera unit was turned on and off manually, but the filming sequence was automatic. It was programmed as follows:

1. Three frames were exposed while the camera was oriented in an upstream direction.
2. The camera was rotated to face at right angles to the channel.

3. Thirty-six exposures were made at a rate of six per second at half-second intervals—a total of 12 seconds.
4. After 4 minutes the camera was reoriented upstream and the sequence was repeated.

The Haines Creek project was discontinued for several reasons after the Santa Anita Wash observations were made. As already mentioned, a continuing drought during the testing phase afforded few runoff events to observe, and therefore the equipment could not be thoroughly tested. Furthermore, the Santa Anita Wash test provided an opportunity to study excellent data which might be years in coming at the Haines Creek site. After observing the flow at Santa Anita Wash and analyzing the data, the author concluded that the programmed sequence from the camera would not provide adequate documentation for determining discharge. Also, the manual on-off switch was a serious shortcoming. An automatic triggering mechanism in the channel was needed to activate the camera when flow reached a significant magnitude. The absence of such a device resulted in the loss of data when an observer was unable to reach the site during a period of flow.

DESCRIPTION OF CONTROLLED TEST IN SANTA ANITA WASH

The Santa Anita Wash flood control channel, in which tests were made April 16, 1965, is rectangular in cross section and is concrete lined. The geometry of the channel at the three observation sites is given in table 1. The heading "Length of measuring reach" refers to the short reach at each observation site where the travel times of the

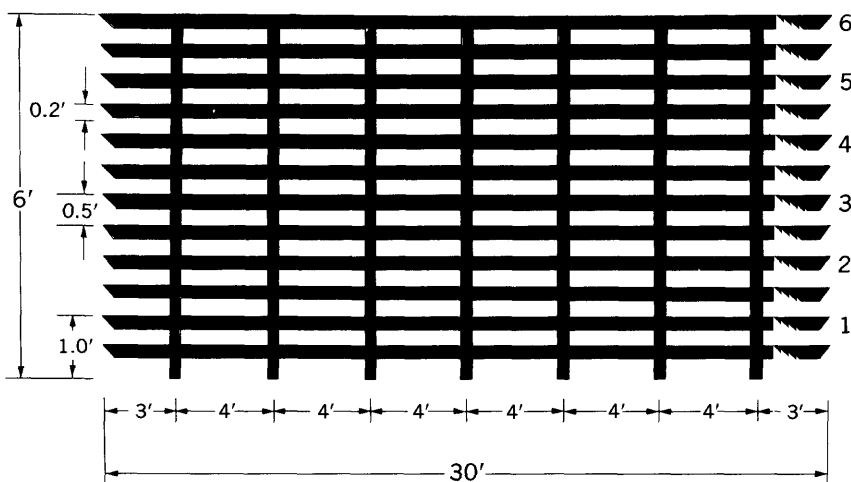


FIGURE 3.—Dimensions and configuration of grid on channel wall.

translatory waves were measured. At each observation site a grid, similar to that shown in figure 3, was painted on the channel wall opposite the observer so that water depths could be read.

TABLE 1.—*Channel geometry at observation sites on Santa Anita Wash flood control channel*

Location of observation site	Length of measuring reach, L_r (ft)	Channel properties		
		Width, b (ft)	Depth (ft)	Slope, S (ft/ft)
Santa Anita Wash above Sierra Madre Wash (O.S. 201)-----	102.5	28.0	11.0	0.0251
Santa Anita Wash at Colorado Blvd. (O.S. 202), 0.78 mile downstream from O.S. 201-----	118.5	30.0	13.0	.0174
Santa Anita Wash at Longden Ave. (O.S. 203), 2.42 miles downstream from O.S. 202-----	115.5	35.0	14.5	.0092

Water was released into the channel from the reservoir at Big Santa Anita Dam (fig. 1), 2.2 miles upstream from O.S. 201, at controlled rates of about 100, 200, and 300 cfs. These discharges were modified by storage in the Santa Anita debris basin, 1.0 mile upstream from O.S. 201, with the result that the discharge hydrograph for the flood control channel did not show abrupt changes in discharge, but instead took the shape shown in figure 4. The discharge hydrographs in figures 4, 5, and 6 were constructed from current-meter discharge measurements made continuously during the test on the crest of the debris-basin dam. Adjustments for travel time from the dam to each observation site were made on the basis of staff-gage observations made at all sites throughout the test. Because of storage in the concrete channel there may be some error in time and discharge in figures 4-6 during the three steep rises and the steep fall of the hydrographs. Storage, however, should have only negligible effect on the three plateaus of nearly steady flow. There was no inflow into the channel from Sierra Madre Wash, which joins Santa Anita Wash a short distance downstream from O.S. 201 (fig. 1).

Figure 7 is a schematic sketch of the water-surface profile in the flood-control channel and lists the elements observed at each observation site. Water depths, as mentioned, were read on the painted grids, and travel times were obtained by stopwatch. Observations were made at intervals of approximately 15 minutes, at which time depths and travel time characteristics were recorded for each of five consecutive waves. In addition, floats were thrown into the channel at varying distances behind the wave crests and their passage through the reach was timed. The floats traveled at approximately the same velocity as the

wave crests at O.S. 201, a result that was not surprising because the waves tended to maintain their spacing and shape in the reach of channel between the upstream bend and Sierra Madre Wash. At O.S. 202 and O.S. 203 observed float velocities were slightly slower than wavecrest velocities. No observations of velocity were made at depths corresponding to D_1 in figure 7. Further documentation of flow character-

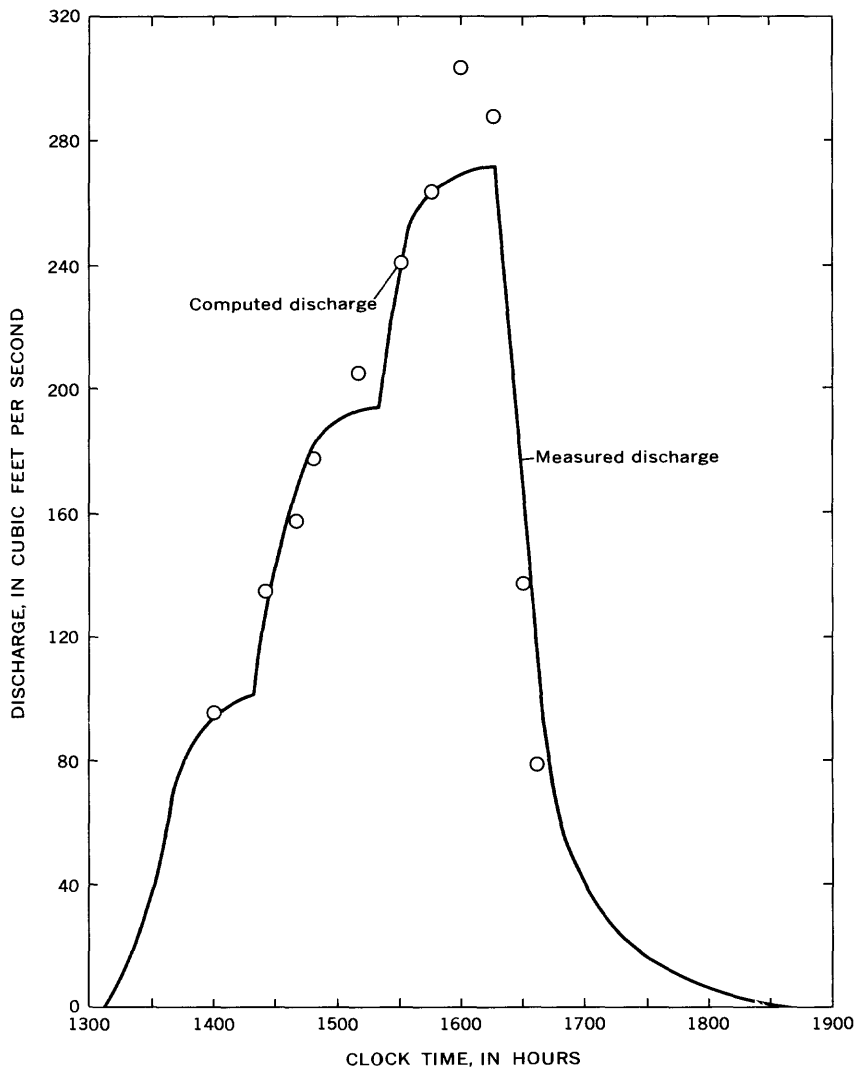


FIGURE 4.—Discharge hydrograph at Santa Anita Wash above Sierra Madre Wash. (O.S. 201) April 16, 1965, and plot of discharges computed from observations of flow.

istics was obtained in motion pictures and still photographs of the flow.

Motion pictures, as well as graphs of observed water depths plotted against time, showed that the longitudinal profile of the waves was slightly concave upward. To simplify the computation of discharge, however, the waves were assumed to have a simple wedge shape, as illustrated in figure 7. For each wave, the dimensions of the wedge were chosen so as to match closely the shape and volume of water in the wave.

METHOD OF COMPUTING DISCHARGE

The method for computing discharge comprised the following steps:

1. Computation of discharge in the overriding wave (Q_w).

The volume of water in the overriding wave was computed, and this volume was divided by the average period of the wave (T_p) to obtain the discharge.

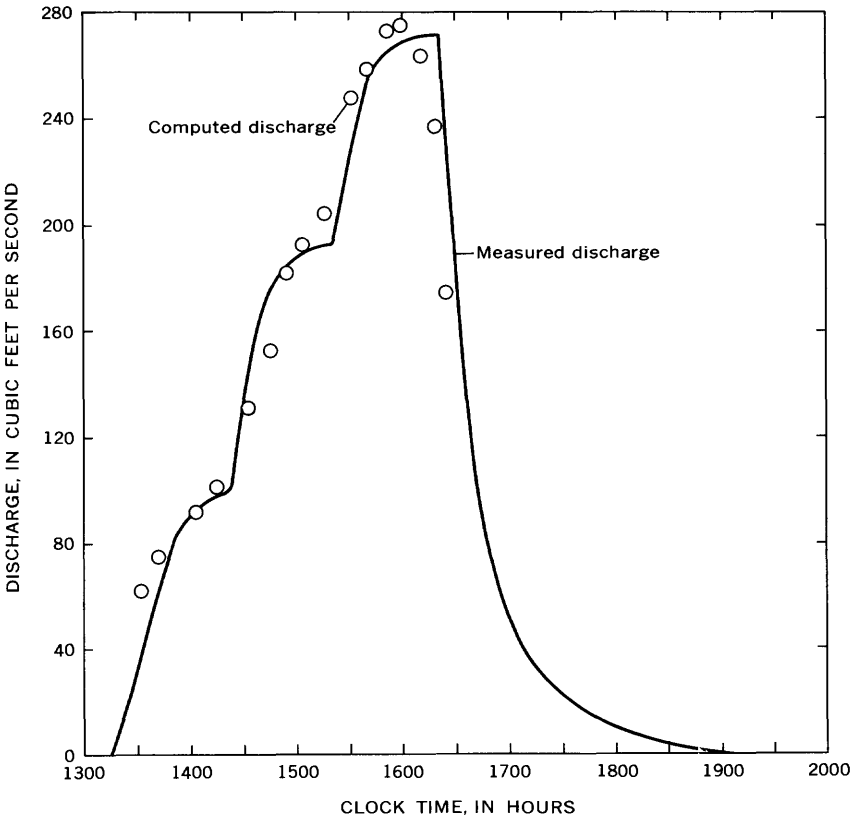


FIGURE 5.—Discharge hydrograph at Santa Anita Wash at Colorado Blvd. (O.S. 202) April 16, 1965, and plot of discharges computed from observations of flow.

2. Computation of discharge in the shallow-depth, or overrun, part of the flow (Q_1).

The product of the depth (D_1) and the width of channel (b) was multiplied by a derived velocity to obtain the discharge.

3. Computation of total discharge.

Total discharge was computed by adding the discharges determined in steps 1 and 2.

The method is explained by reference to the computations for O.S. 201 in tables 2 and 3. No computations were attempted where values of D_1 were less than 0.2 foot, because of the difficulty of getting reliable depth observations at such shallow flows.

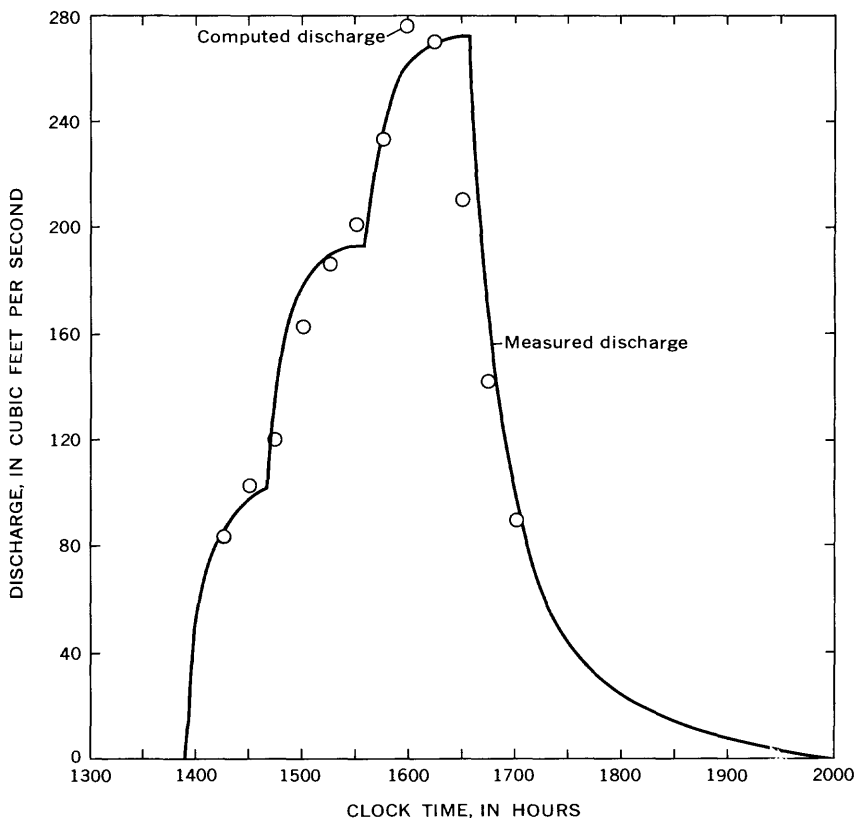


FIGURE 6.—Discharge hydrograph at Santa Anita Wash at Longden Ave. (O.S. 203) April 16, 1965, and plot of discharges computed from observations of flow.

The first six columns of table 2 represent observed data. These observations, other than clock time, were subject to random error because the height of a fluctuating water surface is difficult to read against a coarse grid. Consequently, average values of depth and time for each sequence of five waves were plotted against time of observation, and the plotted points were averaged with a smooth curve. The values for each element in columns 2-6, corresponding to clock time in the first column, were picked from the curves and recorded in table 2. Values of

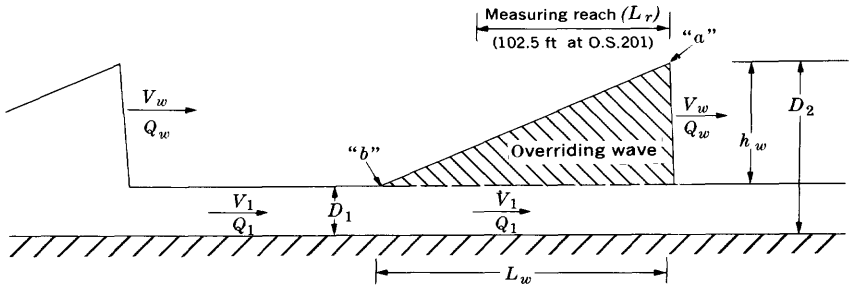


FIGURE 7.—Schematic sketch of longitudinal water-surface profile and list of elements observed.

Elements observed :

D_1 =depth between waves (ft).

D_2 =depth at wave front (ft).

T_p =time interval between arrivals of consecutive wave fronts at observation point (sec).

t_b =time interval between arrivals of crest "a" and trough "t" at observation point (sec).

t_w =time required for wave crest "a" to travel length of measuring reach (sec). For example, length of measuring reach at O.S. 201 is 102.5 ft.

TABLE 2.—Computation of discharge in the overriding wave (Q_w) at O.S. 201

Column 7= $L_r \div$ column 6

Column 8=Column 5 \times column 7

Column 9=Column 3 - column 2

Column 10= $b/2 \times$ column 8 \times column 9

Column 11=Column 10 \div column 4

(1) Clock time (hr)	(2) D_1 (ft)	(3) D_2 (ft)	(4) T_p (sec)	(5) t_b (sec)	(6) t_w (sec)	(7) V_w (fps)	(8) L_w (ft)	(9) h_w (ft)	Overriding wave	
									(10) Volume (ft ³)	(11) Q_w (cfs)
1400	0.20	0.76	15.0	6.0	6.1	16.8	101	0.56	792	53
1424	.23	.85	13.8	6.6	5.4	19.0	125	.62	1,085	79
1440	.24	.90	13.0	7.0	5.2	19.7	138	.66	1,275	98
1450	.25	.92	12.3	7.2	5.0	20.5	148	.67	1,388	113
1510	.25	.97	11.4	7.5	4.8	21.4	160	.72	1,613	141
1530	.26	1.01	10.2	7.5	4.6	22.3	167	.75	1,754	172
1543	.30	1.04	9.7	7.3	4.5	22.8	166	.74	1,720	177
1600	.42	1.08	9.6	6.8	4.4	23.3	158	.66	1,460	152
1614	.45	1.07	9.9	6.2	4.7	21.8	135	.62	1,172	118
1627	.28	.78	12.6	5.6	5.4	19.0	106	.50	742	59
1638	.20	.71	15.0	4.2	6.2	16.5	69	.51	493	33

t_w in column 6 are an average of the observed travel times of several floats through the measuring reach.

Columns 7-11 of table 2, together with the headnotes, illustrate the computation of discharge in the overriding wave (Q_w). V_w , in column 7, is the velocity of the wave through the 102.5-foot measuring reach. The dimensions of the wedge-shaped wave are L_w (column 8), h_w (column 9), and the width of the channel (b) at O.S. 201, which is 28.0 feet. In column 10 these three dimensions were combined to give the volume of water in the wave, and in column 11 the computed volumes were combined with the wave period (T_p) to give the discharge in the overriding wave.

TABLE 3.—Computation of discharge in the shallow-depth (overrun) part of flow (Q_1) and total discharge at O.S. 201

(1) Clock time (hr)	(2) D_1 (ft)	(3) A_1 (ft ²)	(4) Wave celerity (fps)	(6)			(9)		
				V_1 (fps)	Q_1 (cfs)	Total discharge (cfs)	V_1 (fps)	Q_1 (cfs)	Total discharge (cfs)
1400	0.20	5.6	7.7	9.1	51	104	8.0	45	98
1424	.23	6.4	8.0	11.0	70	149	8.7	56	135
1440	.24	6.7	8.3	11.4	76	174	9.0	60	158
1450	.25	7.0	8.3	12.2	85	198	9.2	64	177
1510	.25	7.0	8.7	12.7	89	230	9.2	64	205
1530	.26	7.3	8.9	13.4	98	270	9.4	69	241
1543	.30	8.4	8.7	14.1	118	295	10.4	87	264
1600	.42	11.8	7.9	15.4	182	334	12.9	152	304
1614	.45	12.6	7.6	14.2	179	297	13.5	170	288
1627	.28	7.8	6.9	12.1	94	153	10.0	78	137
1638	.20	5.6	7.2	9.3	52	85	8.0	45	78

Table 3 illustrates the computation of discharge in that part of the flow that is overrun by the translatory waves. The accuracy of the computed values is open to question because water is not an ideal (nonviscous) fluid and the transfer of momentum across streamlines causes the shallow-depth velocities (V_1) to be affected by the velocity of the translatory waves. Column 2 of table 3 lists depths (D_1), and in column 3 these depths have been multiplied by the width of the channel (b) to give the cross-sectional area (A_1). The velocity, V_1 , was determined by two methods. First, the theoretical celerities of the wave fronts, or velocities of the waves relative to V_1 , were determined from the equation for a rectangular channel:

$$\text{Wave celerity} = \sqrt{(g/2)(D_2/D_1)(D_2 + D_1)}$$

where g is the acceleration of gravity. These wave celerities, shown in column 4 of table 3, were subtracted from observed wave velocities,

V_w , obtained from table 2. The differences, representing the theoretical velocities of the shallow-depth part of the flow (V_1), are listed in column 5. Column 6 lists the shallow-depth discharges (Q_1) corresponding to values of V_1 , and in column 7 these discharges were added to the previously computed wave discharges (Q_w) to give total discharge.

The computed total discharges in column 7 are much larger than the discharges shown by the hydrograph in figure 4. Because there was little likelihood of serious error in the determination of discharge in the overriding wave (Q_w), another method of computing the shallow-depth part of the flow (Q_1) was tried. In this second trial, V_1 was computed from the Manning equation:

$$V_1 = (1.486/n)S^{1/2}R^{2/3}$$

where n is the roughness coefficient, S is the slope, and R is the hydraulic radius. Column 8 of table 3 gives the values of V_1 computed from the Manning equation, and columns 9 and 10 show the corresponding values of Q_1 and total discharge. The computed values of total discharge from column 10 have been plotted in figure 4; they fit the hydrograph satisfactorily.

Similar computations of discharge were made for O.S. 202 (tables 4 and 5) and O.S. 203 (tables 6 and 7). At these sites the values of V_1 determined from the celerity equation were much too low to give total discharges that matched the hydrographs in figures 5 and 6. When values of V_1 computed by the Manning equation were used, satisfactory results were obtained. The total discharges obtained in the second trial computations are plotted in figures 5 and 6.

TABLE 4.—*Computation of discharge in the overriding wave (Q_w) at O.S. 202*

Column 7 = $Lr \div$ column 6
 Column 8 = Column 5 \times column 7
 Column 9 = Column 3 - column 2

Column 10 = $b/2 \times$ column 8 \times column 9
 Column 11 = Column 10 \div column 4

(1) Clock time (hr)	(2) D_1 (ft)	(3) D_2 (ft)	(4) T_p (sec)	(5) t_b (sec)	(6) t_w (sec)	(7) V_w (fps)	(8) L_w (ft)	(9) h_w (ft)	(10) Overriding wave		(11) Q_w (cfs)
									Volume (ft ³)		
1333	0.25	0.38	38.0	8.4	12.5	9.5	80	0.13	156	4	
1340	.27	.52	32.0	7.8	11.0	10.8	84	.25	315	10	
1405	.30	.60	26.2	7.4	9.7	12.2	90	.30	405	15	
1415	.31	.62	24.8	7.6	8.8	13.5	102	.31	474	19	
1435	.35	.75	22.8	8.1	8.1	14.6	118	.40	708	31	
1446	.39	.85	22.0	8.4	7.7	15.4	129	.46	890	40	
1456	.41	.96	21.2	8.7	7.6	15.6	135	.55	1,110	52	
1505	.42	.99	20.5	8.8	7.5	15.8	139	.57	1,190	58	
1512	.44	1.00	20.0	9.0	7.4	16.0	144	.56	1,210	60	
1530	.50	1.05	19.0	9.3	7.1	16.7	155	.55	1,280	67	
1539	.51	1.08	18.8	9.4	7.0	16.9	159	.57	1,360	72	
1550	.52	1.10	18.8	9.6	6.7	17.7	170	.58	1,480	79	
1557	.52	1.11	19.0	9.8	6.7	17.7	173	.59	1,530	81	
1609	.51	1.10	21.0	10.0	6.6	18.0	180	.59	1,590	76	
1617	.48	1.03	23.0	10.8	6.8	17.4	188	.55	1,550	67	
1625	.40	.95	30.0	11.8	8.0	14.8	175	.55	1,440	48	

DISCUSSION OF RESULTS

The method of computing total discharge values from the wave discharge and Manning's equation gave results that fit the measured-discharge hydrograph fairly well. A value of $n=0.010$ was used in the Manning equation. This value was calculated by the Los Angeles County Flood Control District (written commun., 1966) using float velocities determined from motion pictures taken during the Santa

TABLE 5.—*Computation of discharge in the shallow-depth (overrun) part of flow (Q_1) and total discharge at O.S. 202*

Column 2=Column 2, table 4 Column 3= $b \times$ column 2 Column 4= $\sqrt{(g/2)(D_2/D_1)(D_1+D_2)}$ Column 5=Column 7, table 4 - column 4 Column 6=Column 3 \times column 5 Column 7=Column 6 + column 11, table 4 Column 8= $(1.486/n)S^{1/2}R^{2/3}$ Column 9=Column 3 \times column 8 Column 10=Column 9 + column 11, table 4									
(1)	(2)	(3)	(4)	(5)	(6) (7) (8)			(9) (10)	
Clock time (hr)	D_1 (ft)	A_1 (ft ²)	Wave celerity (fps)	First trial			Second trial		
				V_1 (fps)	Q_1 (cfs)	Total discharge (cfs)	V_1 (fps)	Q_1 (cfs)	Total discharge (cfs)
1333	0.25	7.5	3.9	5.6	42	46	7.7	58	62
1340	.27	8.1	5.0	5.8	47	57	8.1	66	76
1405	.30	9.0	5.4	6.8	61	76	8.7	78	93
1415	.31	9.3	5.5	8.0	74	93	8.8	82	101
1435	.35	10.5	6.2	8.4	88	119	9.6	101	132
1446	.39	11.7	6.6	8.8	103	143	9.7	114	154
1456	.41	12.3	7.2	8.4	103	155	10.6	130	182
1505	.42	12.6	7.3	8.5	107	165	10.8	136	194
1512	.44	13.2	7.3	8.7	115	175	11.1	146	206
1530	.50	15.0	7.2	9.5	142	209	12.1	182	249
1539	.51	15.3	7.4	9.5	145	217	12.2	187	259
1550	.52	15.6	7.4	10.3	161	240	12.4	194	273
1557	.52	15.6	7.5	10.2	159	240	12.4	194	275
1609	.51	15.3	7.5	10.5	161	237	12.2	187	263
1617	.48	14.4	7.2	10.2	147	214	11.8	170	237
1625	.40	12.0	7.2	7.6	91	139	10.5	126	174

TABLE 6.—*Computation of discharge in the overriding wave (Q_w) at O.S. 203*

Column 7= $L_w \div$ column 6 Column 8=Column 5 \times column 7 Column 9=Column 3 - column 2 Column 10= $b/2 \times$ column 8 \times column 9 Column 11=Column 10 \div column 4										
(1)	(2)	(3)	(4)	(5)	(6)	(7)	(8)	(9)	(10)	(11)
Clock time (hr)	D_1 (ft)	D_2 (ft)	T_p (sec)	t_b (sec)	t_w (sec)	V_w (fps)	L_w (ft)	h_w (ft)	Overriding wave	
									Volume (ft ³)	Q_w (cfs)
1415	0.30	0.56	43	17.0	11.5	10.0	170	0.26	775	18
1430	.33	.62	45	21.0	11.0	10.5	220	.29	1,123	25
1445	.35	.72	48	23.5	10.5	11.0	258	.37	1,677	35
1500	.43	.85	50	25.0	10.0	11.6	290	.42	2,131	43
1515	.47	.90	51	26.5	9.6	12.0	318	.43	2,397	47
1530	.50	.92	54	27.5	9.2	12.6	346	.42	2,557	47
1545	.55	1.01	55	28.0	8.8	13.1	367	.46	2,957	54
1600	.60	1.15	55	28.0	8.3	13.9	389	.55	3,757	68
1615	.58	1.15	52	27.5	8.3	13.9	382	.57	3,810	73
1630	.50	.95	49	25.0	9.2	12.6	315	.45	2,767	56
1645	.40	.74	44	21.0	10.6	10.9	229	.34	1,607	36
1700	.30	.57	40	19.0	12.2	9.5	180	.27	945	24

Anita Wash tests. The float velocities were corrected to mean velocity by assuming the velocity varied directly with the logarithm of the distance from the channel bottom. A higher value of n would give a slightly better fit of computed values to the measured hydrograph during the highest discharges at O.S. 201; however, the results of computations at O.S. 202 and O.S. 203 seem to support the use of $n=0.010$.

As stated earlier, the observed values of flow used to compute discharge were selected from curves determined by plotting average dimension and velocity values of each five-wave sequence against time of observation. The author recognized that a sum of discharge computations for each wave of the sequence would probably give more accurate results, but the data collected were not of sufficient detail or accuracy to permit this approach.

The inconsistent results obtained when the equation for wave celerity was used to compute the velocity at minimum depth (V_1) is probably due to the fact that the celerity equation is valid only when the flow is uniform on each side of the wave front. Uniformity does not exist upstream from the wave front during pulsating flow.

The observed wave characteristics at the three observation sites at the approximate time of maximum discharge are shown in table 8. The most striking difference is in the wave velocity.

TABLE 7.—*Computation of discharge in the shallow-depth (overrun) part of flow (Q_1) and total discharge at O.S. 203*

Column 2=Column 2, table 6 Column 3=b X column 2 Column 4= $\sqrt{(g/2)(D_2/D_1)(D_2+D_1)}$ Column 5=Column 7, table 6 - column 4 Column 6=Column 3 X column 5				Column 7=Column 6 + column 11, table 6 Column 8=(1.486/n) $S^{1/2}R^{2/3}$ Column 9=Column 3 X column 8 Column 10=Column 9 + column 11, table 6					
(1)	(2)	(3)	(4)	(5) (6) (7)			(8) (9) (10)		
Clock time (hr)	D_1 (ft)	A_1 (ft ²)	Wave celerity (fps)	First trial			Second trial		
				V_1 (fps)	Q_1 (cfs)	Total discharge (cfs)	V_1 (fps)	Q_1 (cfs)	Total discharge (cfs)
1415	0.30	10.5	5.1	4.9	51	69	6.3	66	84
1430	.33	11.6	5.4	5.1	59	84	6.7	78	103
1445	.35	12.2	6.0	5.0	61	96	7.0	85	120
1500	.43	15.0	6.4	5.2	78	121	8.0	120	163
1515	.47	16.4	6.5	5.5	90	137	8.5	139	186
1530	.50	17.5	6.5	6.1	107	154	8.8	154	201
1545	.55	19.2	6.8	6.3	121	175	9.4	180	234
1600	.60	21.0	7.4	6.5	136	204	9.9	206	276
1615	.58	20.3	7.4	6.5	132	205	9.7	197	270
1630	.50	17.5	6.7	5.9	103	159	8.8	154	210
1645	.40	14.0	5.8	5.1	71	107	7.6	107	143
1700	.30	10.5	5.2	4.3	45	69	6.3	66	90

TABLE 8.—*Observed wave characteristics at approximate time of maximum discharge*

Observation site	Time of observation (hr)	Depth between waves, D_1 (ft)	Depth at wave front, D_2 (ft)	Wave velocity, V_w (fps)
Santa Anita Wash above Sierra Madre Wash (O.S. 201)-----	1600	0.5	1.1	23.3
Santa Anita Wash at Colorado Blvd. (O.S. 202)-----	1609	.5	1.1	18.5
Santa Anita Wash at Longden Ave. (O.S. 203)-----	1615	.6	1.1	13.9

In summary, the methodology used to determine the discharge of pulsating flow is adequate, but more accurate observations would improve the discharge computation. In the following section two methods are described for recording the elements necessary to determine discharge during pulsating flow by the method developed in this study. A third method that has some promise for determining the discharge is the dye-dilution method. It is also briefly discussed in the section that follows.

PROPOSED METHODS OF DETERMINING DISCHARGE

PHOTOGRAPHIC METHOD

Discharges may be determined from measurements of channel geometry and observations of wave velocity and shape, maximum depth, and minimum depth, as shown in the Santa Anita Wash test. Tests of the robot camera at Haines Creek have shown that the programmed sequence used at that site was inadequate to define all the elements needed. Following is a brief description of the filming sequence and equipment necessary to determine discharges from motion pictures. A schematic sketch, shown in figure 8, gives the general component layout. The operating sequence is as follows:

1. Unit is turned on automatically when minimum water level is maintained at some preselected depth. The time the unit is turned on is recorded on a clock-driven chart.
2. A power-driven 16-mm camera, with automatic electric-eye diaphragm, operates for 180 seconds at a rate of 10 frames per second. Floodlights and a timing light operate simultaneously with the camera.
3. After 15 minutes, the sequence is repeated.
4. When minimum water level recedes below the preselected depth, the unit is shut off automatically and the time is recorded on the clock-driven chart.

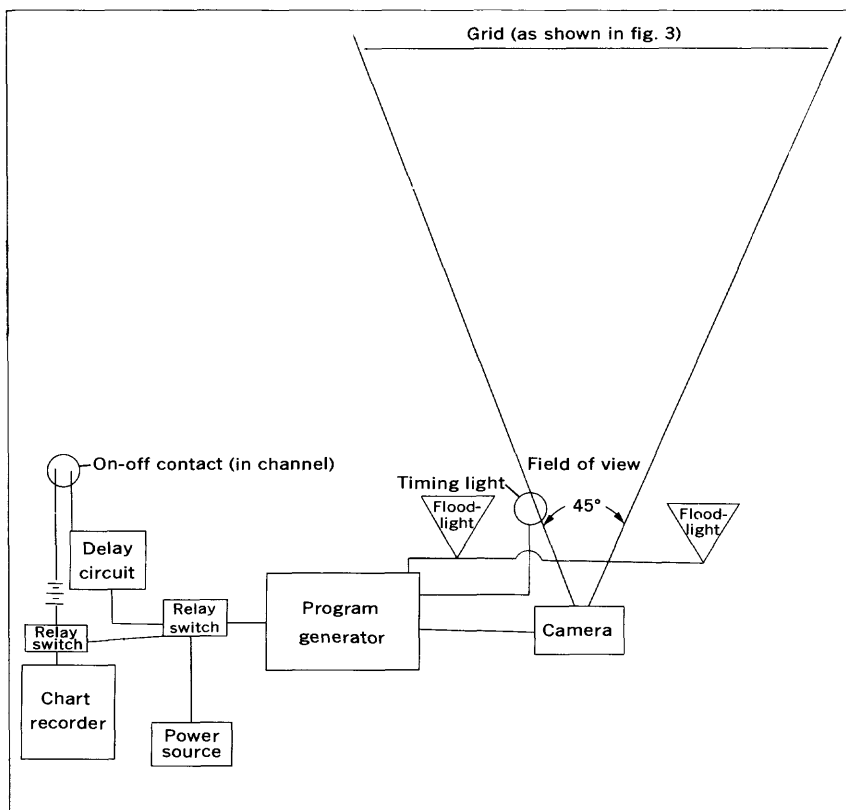


FIGURE 8.—Schematic sketch of general component layout for photographic method of determining discharge.

The automatic on-off switch consists of a pair of contacts, set at a predetermined depth and connected to a relay switch which closes when the contacts are submerged. A delay unit between the contacts and the relay switch prevents a fluttering of the power to the sequence unit when the water level is fluctuating near the depth of the contacts. The time on and off is marked on a clock-driven chart with the aid of a second relay switch attached to a marking pen. When the relay switch is closed, the sequence unit supplies power to the floodlights, timing light, and camera for 180 seconds every 15 minutes. This allows filming of at least five waves with an average period of 36 seconds or less. The timing light, set in the field of view of the camera, will flash for 0.2 second every 10 seconds to aid in determining the exact number of frames per second exposed. There are 40 frames per foot of 16-mm film; the film required for 4 hours of operation (3 minutes every 15 minutes) is 720 feet. Magazines up to 900 feet are available for some cameras.

The floodlights, which are necessary for filming at night, require a high power source for operation. Therefore, a large rechargeable battery pack or, preferably, line power is required.

A frame-by-frame analysis of each wave will yield wave-front velocity and wave dimensions, including maximum and minimum depth. If debris is present, surface velocities at various points behind the wave front may also be determined. Discharge for each wave is computed separately and then averaged for the five-wave sequence.

DEPTH-RECORDER METHOD

The depth recorder is an analog device which transforms electrical current received from a depth-sensing unit to a measure of the corresponding depth of water. The depth-sensing unit consists of several electrical contacts set at known intervals above the channel bottom. When the lowest contact is submerged, a connecting relay switch is closed, the unit is turned on, and a known amount of current is supplied to an analog recorder. As more contacts are submerged, more current is supplied. The recorder is calibrated so that incoming current is proportional to depth of water. The resultant depth of water is plotted against time on moving graph paper. A magnetic-tape recorder in parallel with the graphic recorder would facilitate data analysis with a digital computer. The time on and off are each recorded on the chart.

Analysis of data from a single depth sensor would yield a graph of stage only. To determine wave velocity and compute wave shape, a second sensor is installed at a known distance downstream from the first. Data from both sensors are recorded simultaneously. The velocity of the wave is equal to the distance between sensors divided by the wave travel time.

An a-c power supply would be preferable to battery power to prevent polarization of the contacts on the depth sensor.

DYE-DILUTION METHOD

The Geological Survey and others have successfully measured the discharge of stable flow by injecting dye of a known concentration into a stream at a constant rate.¹ Downstream from the injection site, at a distance sufficiently long to allow complete mixing of the dye and water, samples of the water are taken. The dye concentrations of the samples are determined by fluorometer, and a simple computation gives the discharge of the stream. Studies by F. A. Kilpatrick of the

¹ Cobb, E. D., and Bailey, J. F., 1965. Measurement of discharge by dye-dilution methods: unpub. data to be published as Techniques of Water Resources Investigations of the U.S. Geological Survey.

Geological Survey (written commun., 1966) have shown that the process can be automated to obtain continuous measurement of discharge, but no automatic dye-injection equipment is operational at this time.

Three types of automatic samplers may be used. Two types are operational; they are the individual-sample bottling system (U.S. Inter-Agency Committee on Water Resources, 1963, p. 124) and a chart-recorder assembly (such as that made by G. K. Turner Associates, Palo Alto, Calif.) connected to an open-door flow-through fluorometer. Both require line or battery power. The third type, being developed at Colorado State University by T. M. Zorich (written commun., 1966), shows considerable promise for use in isolated sites. Dye is injected to the stream at a constant rate using a Mariotte vessel. After the dye and water are well mixed, water is diverted from the channel by gravity flow past a capillary-feed stylus. The stylus applies a sample of the water to a clock-driven roll of filter paper, and the filter paper is later processed through a fluorometer. The last two methods provide a continuous recording of dye concentration.

There is some question as to how successful the dye-dilution method would be for measuring pulsating flow. In the Santa Anita Wash flood control channel, the method would undoubtedly be successful if the dye were injected and sampled upstream from the bend where the translatory waves become fully developed. However, its success there would not prove the general applicability of the method in a channel carrying pulsating flow. The method should be tested under controlled-flow conditions, similar to those of April 16, 1965, by the injection of dye downstream from the above-mentioned bend in the Santa Anita Wash channel.

DISCUSSION OF PROPOSED METHODS

Successful analysis of motion picture data from the Santa Anita Wash test has shown that discharge during pulsating flow can be computed by the photographic method. The proposed instrumentation has some limitations which should be considered when selecting a method. The system is complex, and when it is operating under field conditions, regular maintenance and testing would be required to prevent failure of any component. The small film magazine capacity precludes a continuous monitoring of the flow and during prolonged flow, film must be replaced frequently. Hence, the method is not adaptable for use in isolated areas. Frame-by-frame analysis of the film to determine discharge is tedious and time consuming.

As for the depth-recorder method, the depth-sensing part of the analog recorder has not been developed and tested. Providing that this part of the system can be made operational, this method has certain

obvious advantages over the photographic method. Stage is continuously recorded in a form that can be easily analyzed—not in 15-minute samples, as in the photographic method. Since the contacts are exposed in the channel, regular testing and maintenance would be required. The system requires line power which may prevent its use in isolated areas.

The dye-dilution method has not been tested during pulsating flow. Should the method prove successful, computations of discharge from the measurement of dye concentration are simple and direct. The dye-dilution method is the only method of the three discussed which does not require line power for operation except when the sampling is done with a continuous-recording flow-through fluorometer; it is therefore adaptable to field use at isolated sites. The dye-dilution method may not be applicable in smooth channels during high flows when pulsating flow is not fully developed and the turbulence is low; the channel may not be long enough for adequate mixing of the dye. The length of channel necessary for adequate mixing of the dye would increase if the turbulence decreased for any reason. This might occur, for example, if pulsating flow became less pronounced with an increase in discharge. If the distance for adequate mixing is such that tributary inflow between the points of dye injection and sampling is significantly large, the method cannot be used.

SUMMARY AND CONCLUSIONS

A method of determining the discharge during pulsating flow was tested in the Santa Anita Wash flood control channel in Arcadia, Calif., April 16, 1965. Observations of the dimensions of the transitory waves and of the velocity of the wave fronts were made at three sites during a period of known discharges ranging from 0 to 270 cfs. The method of computing discharge was based on (1) computation of the average discharge of the overriding wave, as determined from its observed volume and period, and (2) computation of the discharge in the shallow-depth, or overrun, part of the flow, the velocity of which was determined from the Manning equation. The method gave satisfactory results. The procedure used—separating the flow into two components and then treating the shallow-depth component as though it were steady—has no theoretical basis. It is, however, an expedient for use until laboratory investigation can provide a satisfactory analytical solution to the problem of computing discharge during pulsating flow.

Earlier, a robot camera had been designed and programed to obtain the data needed to compute discharge by the method described above. The photographic equipment had been installed in Haines Creek flood control channel, but it had not been completely tested because of the

infrequency of flow in that channel. Because of a prolonged drought at Haines Creek and because the Santa Anita Wash tests demonstrated the inadequacy of the operating sequence of the camera, development of the camera technique was discontinued at the Haines Creek site.

Three methods are proposed for obtaining the data needed to compute discharge during pulsating flow. Two of them—the photographic method and the depth-recorder method—are based on observations of wave size, shape, and velocity. From these observations the discharge is computed by the procedure described above. The third method proposed—discharge determination by dye dilution—is based on the relation between rate of flow and measured dye concentration at a site downstream from a point of constant-rate injection. Each method has limitations which must be considered when selecting instrumentation for determining discharge during pulsating flow.

Each of the three methods proposed for determining discharge during pulsating flow should be developed and tested under conditions similar to those in the Santa Anita Wash test of April 16, 1965.

SELECTED REFERENCES

- Chow, Ven Te, 1959, *Open-channel hydraulics*: New York, McGraw-Hill, 680 p.
- Craya, A., 1952, The criterion for the possibility of roll-wave formation in Gravity waves: Natl. Bur. Standards Circ. 521, p. 141–151.
- Dressler, R. F., 1949, Mathematical solution of the problem of roll waves in inclined open channels: *Commun. on Pure and Appl. Mathematics*, v. 2, p. 149–194.
- 1952, Stability of uniform flow and roll-wave formation, in *Gravity waves*: Natl. Bur. Standards Circ. 521, p. 237–241.
- Escoffier, F. F., and Boyd, M. B., 1962, Stability aspects of flow in open channels: *Am. Soc. Civil Engineers Proc., Hydraulics Div. Jour.*, v. 88, no. HY6, p. 145–166.
- Holmes, W. H., 1936, Traveling waves in steep channels: *Civil Eng.*, v. 6, no. 7, p. 467–468.
- U.S. Inter-Agency Committee on Water Resources, Subcommittee on Sedimentation, 1963, A study of methods used in measurement and analysis of sediment loads in streams; Report 14, Determination of fluvial sediment discharge: 151 p.
- Iwasa, Y., 1954, The criterion for instability of steady uniform flows in open channels: *Kyoto Univ., Mem. Fac. Eng.*, v. 16, no. 4, p. 264–275.
- Koloseus, H. J., and Davidian, Jacob, 1966, Free-surface instability correlations: U.S. Geol. Survey Water-Supply Paper 1592-C, 72 p.
- 1966, Roughness-concentration effects on flow over hydrodynamically rough surfaces: U.S. Geol. Survey Water-Supply Paper 1592-D, 21 p.
- Mayer, P. G., 1959, Roll waves and slug flow in inclined open channels: *Am. Soc. Civil Engineers Proc., Hydraulics Div. Jour.*, v. 89, no. HY4, p. 99–141.
- Powell, R. W., 1948, Vedernikov's criterion for ultra-rapid flow: *Am. Geophys. Union Trans.*, v. 29, no. 6, p. 882–886.
- Thomas, H. A., 1940, The propagation of waves in steep prismatic conduits: *Iowa Univ., Hydraulics Conf. Proc.*, p. 214–229.